Article |

JWST molecular mapping and characterization of Enceladus' water plume feeding its torus

Check for updates

G. L. Villanueva [1] ✉, H. B. Hammel [2], S. N. Milam [1], V. Kofman [1,3], S. Faggi[1,3], C. R. Glein[4], R. Cartwright[5], L. Roth [6], K. P. Hand[7], L. Paganini [8], J. Spencer [9], J. Stansberry [10], B. Holler[10], N. Rowe-Gurney [1,11], S. Protopapa[9], G. Strazzulla[12], G. Liuzzi[13], G. Cruz-Mermy[14], M. El Moutamid[15], M. Hedman[16] & K. Denny[16]

Enceladus is a prime target in the search for life in our Solar System, having an active plume that is likely to be connected to a large liquid water sub-surface ocean. Using the sensitive near-infrared spectograph instrument on board the James Webb Space Telescope, we searched for organic compounds and characterized the plume's composition and structure. The observations directly sample the fluorescence emissions of H_2O and reveal an extraordinarily extensive plume (up to 10,000 km or 40 Enceladus radii) at cryogenic temperatures (25 K) embedded in a large bath of emission originating from Enceladus' torus. Intriguingly, the observed outgassing rate (300 kg s^{-1}) is similar to that derived from close-up observations with Cassini 15 years ago, and the torus density is consistent with previous spatially unresolved measurements with Herschel 13 years ago, which indicates that the vigour of gas eruption from Enceladus has been relatively stable over decadal timescales. This level of activity is sufficient to maintain a derived column density of 4.5×10^{17} m^{-2} for the embedding equatorial torus, and establishes Enceladus as the prime source of water across the Saturnian system. We performed searches for several non-water gases (CO_2, CO, CH_4, C_2H_6, CH_3OH), but none were identified in the spectra. On the surface of the trailing hemisphere, we observe strong H_2O ice features, including its crystalline form, yet we do not recover CO_2, CO or NH_3 ice signatures from these observations. As we prepare to send new spacecraft into the outer Solar System, these observations demonstrate the unique ability of the James Webb Space Telescope to provide critical support for the exploration of distant icy bodies and cryovolcanic plumes.

Enceladus is likely to be the largest source of water within the Saturnian system[1], with H_2O and other materials jetted into Saturn orbit by localized geological activity[2,3]. Early hints of geological activity on Enceladus were provided by Voyager and telescopic observations in the 1980s and 1990s, which found a close association between Saturn's E ring and Enceladus' orbit[4–8]. In 2005, multiple instruments on board the Cassini spacecraft discovered a plume of gases (predominately water vapour) and ice grains emerging from fissures in the south polar region
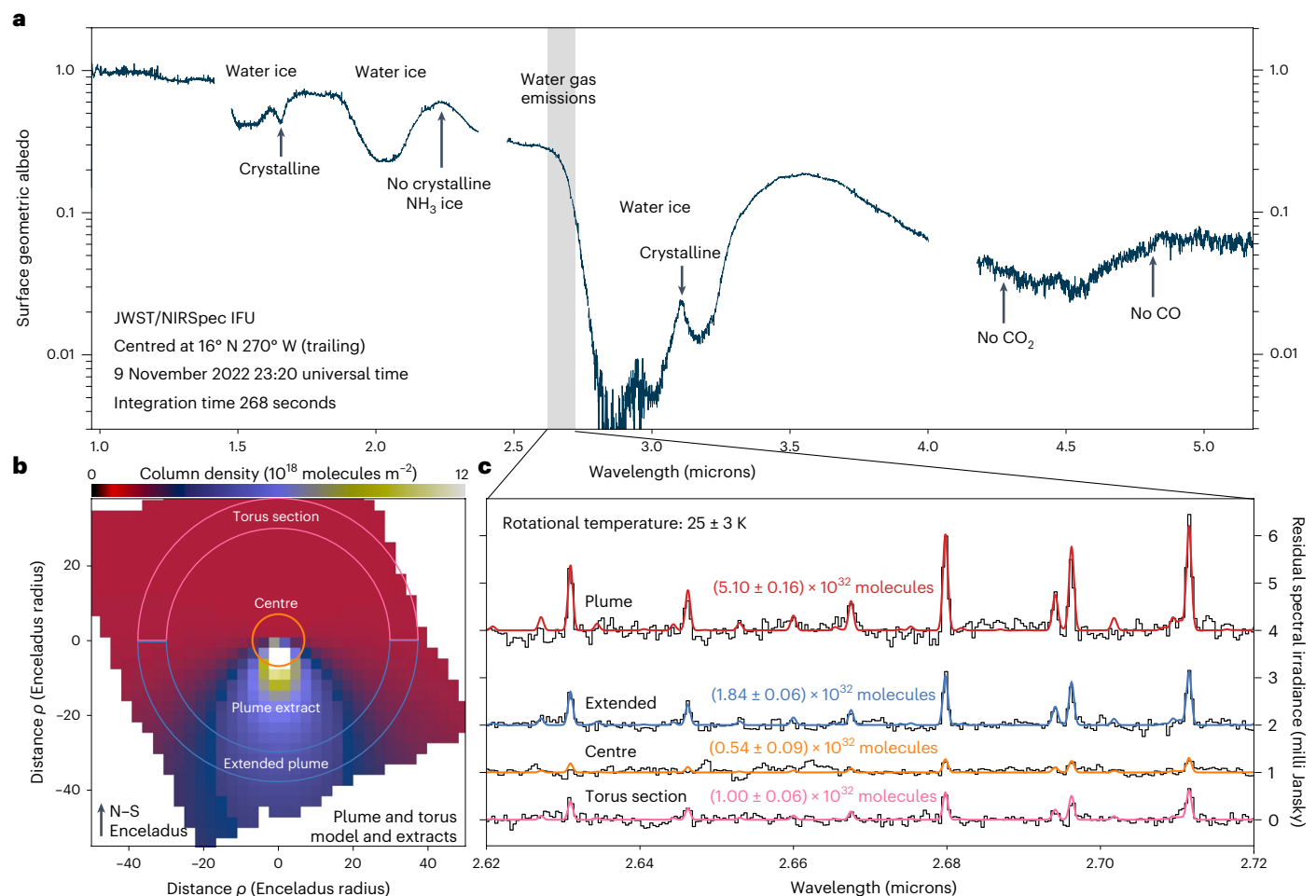
Fig. 1 | Enceladus' surface geometric albedo and detected water vapour emissions. a, Surface geometric albedo of the trailing hemisphere normalized with respect to a reflected solar model[30]. The spectrum shows several strong signatures of H_2O ice, while no absorptions are observed at the expected wavelengths for CO_2, CO or NH_3 ice. **b**, Model of the observed water outgassing, in which four distinct regions are identified: the centre region (orange circle) within seven Enceladus radii (R_E); the inner plume region between 7 R_E and 30 R_E; the extended plume region (blue contour) towards the south and between 30 R_E and 38 R_E; and the torus background region (pink contour) towards the north and between 30 R_E and 38 R_E. **c**, Data (black lines) and model (coloured lines) of the H_2O fluorescence emissions within the four regions of panel **b**, shifted vertically for clarity. The retrieved number of molecules for each region is also indicated. All models are consistent with a rotational temperature of 25 ± 3 K.

of Enceladus[9–14], while a torus of water along Enceladus' orbit was most recently observed via sub-millimetre spectroscopy with the Herschel Observatory[15]. The Cassini measurements of the plume gas were made using in situ mass spectrometry along specific flyby trajectories[16,17] and via stellar occultation in the inner region of the plume (<200 km)[9,18]. In contrast, the sub-millimetre measurements of the torus were not spatially resolved, but they indicated the presence of H_2O gas widely throughout the Saturnian system. While the plume's flux of icy grains varies on multiple timescales[19], the variations in the vapour flux are much less well understood, together with how these affect the structure and evolution of the torus. By analysing the molecular emissions across large distances from Enceladus with the James Webb Space Telescope (JWST)[20], we were able to map the distribution of outgassed water, compare the level of activity with that determined by Cassini measurements and establish a direct connection between the plume and the extended cloud of material beyond the plume that is likely to have accumulated over multiple orbits.

On 9 November 2022 universal time, we observed Enceladus' trailing hemisphere with JWST as part of the Solar System Guaranteed-Time-Observations programme 1250. The James Webb Space Telescope near-infrared spectrograph (JWST–NIRSpec)

observations were made with the integral field unit (IFU)[21], delivering a datacube across three high-resolving power gratings (G140H, G235H, G395H), having two detectors per grating (NRS1, NRS2), with a uniform spaxel size of 0.1″ × 0.1″ across a 3″ × 3″ field of view (FOV)—Enceladus was 0.07″ in diameter at the time of the observations. To minimize saturation, we employed the NRSRAPID readout and short integration times per frame, totalling 215–270 seconds of integration per grating. The data were processed employing the latest version of the JWST Science Calibration Pipeline (v.1.9), and we developed ad hoc algorithms to analyse the frames, combine dithering images and clean bad pixels (scripts publicly available at github.com/nasapsg). In Fig. 1, we present flux-calibrated spectra for the integrated signal across the Enceladus disk and molecular residuals along several regions of the extended plume.

Results
Surface ices
The Enceladus disk spectrum as observed with JWST is dominated by water (H_2O) ice, including its crystalline form (features at 1.65 μm and 3.1 μm), with the main features similar to those identified using Cassini's visible and infrared mapping spectrometer (VIMS)[2] and from
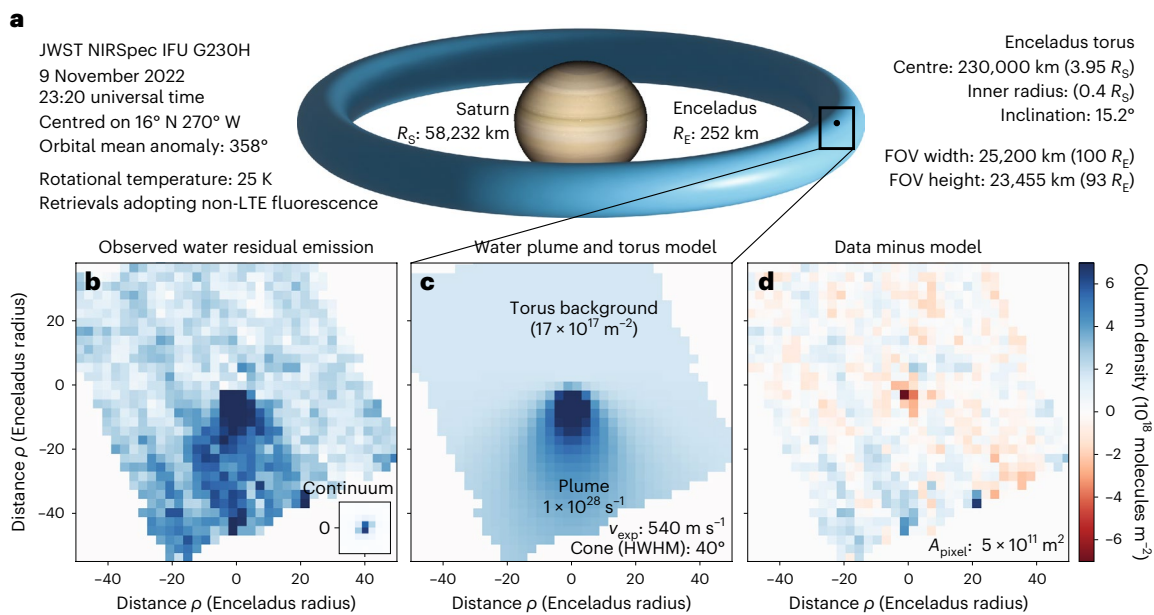
Fig. 2 | Water emission is observed across the whole FOV, revealing an immense water plume and an extended torus. a, The observations sample the trailing hemisphere of Enceladus and the edge of the torus, where R_S refers to the mean radius of Saturn. **b**, At each spaxel (0.1″ × 0.1″), the H_2O column density was retrieved from the observed molecular fluorescence emissions in the 2.62 μm to 2.72 μm range. Enceladus is 0.07″ in diameter (smaller than a spaxel), and the continuum image of the point spread function is shown in the inset box. Some residual diagonal striping is observed, which we suspect originates from detector effects. **c**, A model[30] with two components as shown in Fig. 1b, consisting of a plume and a torus background emission, reproduces the observations well. **d**, A residual image was computed by subtracting the outgassing model from the observations, revealing a close fit to the data.

ground-based observations[22,23]. Carbon dioxide (CO_2) ice features were previously identified near 2.7 μm and 4.3 μm on the surface of Enceladus and primarily at southern polar latitudes (80–90° S) from VIMS[2,24], but in the JWST spectrum we do not identify either of these CO_2 ice bands. The non-detection of CO_2 on Enceladus with JWST is likely to be due to the observing geometry at the time of the observations (centred at 16° N, 270° W), which did not sufficiently sample Enceladus' southern polar regions. This further establishes that CO_2 ice is likely to be confined to the south polar terrain and is probably replenished by plume CO_2 (refs. 2,25). We do observe a potential signature near 4.5 μm, which could be related to CN compounds, yet this identification is only tentative from these data. More information about this and other possible ice identifications is given in the Methods section.

We also searched for ammonia (NH_3) ice, which can strongly depress the freezing point of water and could indicate a sub-surface liquid water reservoir that feeds the plume[17], but we did not identify it in the spectrum (either amorphous or crystalline). Spectroscopic searches for crystalline NH_3 ice in the near infrared have mostly focused on a feature near 2.24 μm, attributed to a combination mode. Ground-based observations of the trailing side of Enceladus detected a subtle band centred near 2.25 μm that was tentatively attributed to NH_3 ice, but other observations obtained in 1995 and 1998 did not display this feature[22]. We did notice a weak and broad feature spanning ~2.15 μm to 2.2 μm that has been attributed to NH_3–H_2O mixtures and ammonium (NH_4)-bearing species on other icy moons[26]. However, this absorption was inconclusive between dithers and was not consistent with the 2.24 μm expected location for NH_3 ice or with the previously detected 2.25 μm feature on Enceladus. Additionally, there is no clear evidence of the ~2.0 μm absorption band due to solid ammonia and its hydrates[27] and expected to overlap with the much stronger 2.0 μm water ice band. We also searched for the stronger NH_3 ice band at 2.96 μm (ref. 28), but the NIRSpec spectra do not show any absorption at this wavelength. Our non-detection of NH_3 ice agrees with the non-detection of surface NH_3 on a global scale by Cassini VIMS[2].

Plume and torus mapping

The uniqueness of JWST for exploring Enceladus is most evident when probing with unparalleled sensitivity the narrow infrared emissions emanating from the plume. Such probing is possible thanks to JWST's very low operational temperatures (~40 K), broad wavelength coverage (0.6 μm to 28.3 μm), large collecting area (25.4 m²), high spectral resolving power (up to $\lambda/\delta\lambda \approx 3{,}000$) and advanced infrared instrumentation (for example, IFU and multi-grating). Infrared gas emissions at these wavelengths are primarily due to solar-pumped fluorescence, so they are particularly weak at these large heliocentric distances. Furthermore, the molecular features are narrow and confined to at most twice the expansion velocity ($v_{exp} \approx 540$ m s^{-1})[1] requiring high-resolution spectroscopy, which is sensitively done with JWST since we can also probe the strong molecular fundamentals of H_2O and CO_2 (not accessible to ground-based observatories due to the lack of atmospheric transparency). Across the Enceladus plume, we detect several strong H_2O molecular emissions (Fig. 1)—also at the spaxel level (Fig. 2)—revealing a highly localized source oriented southward and extending out to at least 10,000 km (40 Enceladus radii (R_E)). We retrieved column densities from the measured line fluxes by employing the publicly available Planetary Spectrum Generator tool at psg.gsfc.nasa.gov (refs. 29,30), which integrates non-local thermodynamic equilibrium (non-LTE) fluorescence radiative-transfer models[31–33] (Methods). From the relative intensities of the water ro-vibrational lines, we determined that the water molecules are at a rotational temperature of $T_{rot} = 25 \pm 3$ K, and this temperature is consistent across the different regions explored (that is, local plume, extended plume and background emission) by our measurements (Fig. 1). These observed temperatures refer to the rotational excitation temperature, not to the ambient kinetic temperature of H_2O vapour. Due to the large extension of the plume and low local densities, this sparse collisional regime dictates that the molecules are no longer in LTE but are in an equilibrium state defined by the insolation rate and the intrinsic probability of absorption or emission of the molecule.

The observed map of water column densities can be relatively well modelled[30] (Fig. 2) when considering an ejecta plume with an outgassing rate of $(1.0 \pm 0.1) \times 10^{28}$ molecules per second (300 kg s^{-1}), a three-dimensional ejecta cone half-width of 40°, as inferred from these data, and an expansion velocity of 540 m s^{-1} (an intermediate value between the ~400 m s^{-1} thermal velocity[3], the vertical velocity of ~600 m s^{-1}, as inferred from near-surface measurements[34], and the ~700 m s^{-1} flow velocities inferred from an outgassing model[16]). This observed level of activity is similar to that inferred from measurements[1,18] made in Saturn's orbit by Cassini 6–19 years ago (1×10^{28} molecules per second), although some other analyses suggest large temporal variability in outgassing from Enceladus[16,35]. We also observe a relatively constant background water emission across the whole FOV with an average column density of $(1.7 \pm 0.1) \times 10^{18}$ m^{-2}. Such emission is most likely to come from water molecules within the torus, which is being observed at the ansa of the orbital path of Enceladus with an inclination of 15.2°. If we assume a constant average density within the torus and zero density outside, and take into account that the torus minor radius or scale height is considerably smaller than its major radius (~237,000 km, centred on Enceladus' orbit), then the equatorial column density (N_T) cutting perpendicularly through the torus centre can be estimated to be $N_T \approx 4.5 \times 10^{17}$ m^{-2} (1.7×10^{18} m^{-2} sin 15.2°). Our measurement is remarkably consistent with that inferred from sub-millimetre observations[15] obtained 13 years ago, which indicated an equatorial column density of 4×10^{17} m^{-2} and a torus scale height of $H_T \approx 25,000$ km.

Discussion

As Enceladus orbits rapidly around Saturn with a period of only 1.37 Earth days, the ejected water vapour is spread along and around its orbit, forming a large torus around Saturn. Considering that the photochemical lifetime[36] of water near Saturn is relatively long (~94 days) and combining this value with the derived production rate of the plume, we estimate that up to 8×10^{34} molecules are available at a given time. Alternatively, and from our derived torus equatorial column density (N_T) and the inferred torus scale height (H_T), we estimate that a total of 2.5×10^{34} molecules are confined within the torus, which is equivalent to 32% of the ejected molecules. This would mean that a large fraction of the ejected H$_2$O molecules (and its OH and O products) are spread beyond the torus and across the Saturnian system. These results generally agree with the findings by Cassidy and Johnson[1], establishing Enceladus as the dominant source of exogenous H$_2$O, OH and O species in the Saturnian system. In addition to H$_2$O vapour, we searched for CO$_2$, CO, CH$_4$, C$_2$H$_6$ and CH$_3$OH molecular emissions across the plume, but none were detected (Extended Data Fig. 1 and Methods). Upper limits (3σ) on their abundances are, respectively, <1%, <10%, <4%, <6% and <20% relative to water. These limits are within the abundances reported from Cassini Ion and Neutral Mass Spectrometer measurements[25,37] of the dense plume region of Enceladus (CO$_2$: 0.3–0.8%, CO < 0.05%, CH$_4$: 0.1–0.3%, C$_2$H$_6$ < 0.2%, CH$_3$OH < 0.01%). Ultraviolet imaging spectrograph occultations also showed no evidence of CO (<1%) in the inner regions of the plume[18]. Our upper limit on the CO$_2$/H$_2$O ratio provides additional support for the idea[38] that extensive CO$_2$ sequestration in Enceladus' rocky core is probably needed to explain why its plume is strongly depleted in CO$_2$ compared with cometary observations[39,40].

Conclusions

These first observations with JWST (only a few minutes of integration time) demonstrate the power of this observatory for sensitively characterizing this ocean world, opening a new window into the exploration of Enceladus' ongoing plume activity while preparing for future missions[41]. More generally, JWST can provide detailed quantitative insights into H$_2$O vapour-dominated geological and cryovolcanic activity elsewhere in the Solar System.

Methods

Retrievals of plume molecular species and derivations of upper limits

To search for narrow molecular features, we analysed the residual spectra which were derived by subtracting a continuum model that included solar Fraunhofer lines from the observed Enceladus spectra. We performed integrations across several regions throughout the environment of Enceladus (Fig. 1) and determined the number of molecules and corresponding column densities. We detect signatures of water vapour in all regions, with the most prominent molecular features and detections across the plume region ($7 < \rho < 30\,R_E$, 0.2″ to 1.0″, 1765 km to 7563 km). This region also has a low intrinsic continuum signature from the Enceladus disk which simplifies the removal of the non-gas signatures. Therefore, we used this region to search for other gases beyond H$_2$O. The fluorescence models are based on non-LTE radiative-transfer modelling[31–33]. Broad non-molecular features were removed by fitting a polynomial function to the continuum shape over the spectral regions presented in Extended Data Fig. 1. Retrievals and the statistical analysis were performed using PSG, in which the retrieval algorithm is based on the optimal estimation method[42]. After each iteration of the retrieval algorithm, a new model was constructed and numerical derivatives were computed for each parameter. This process was repeated until convergence was achieved, and the differences between data and model were minimized. The mean statistical variation of the residual spectra (root-mean-square or chi-square) was used to quantify the uncertainty (sigma) in the retrieved column densities.

Additional findings regarding the characterization of the icy surface of Enceladus

The trailing hemispheric spectrum of Enceladus measured with NIRSpec does show some interesting features, which could provide additional information regarding the composition and physical properties of Enceladus' surface. However these findings are not conclusive at this stage, and additional laboratory experiments, observations, analysis and modelling would be required to further establish the significance of these findings.

Origin of the water crystalline features. The presence of the 1.65 μm and 3.11 μm features that we observe in the Enceladus spectrum (Fig. 1) clearly testifies to the crystallinity of the H$_2$O ice[43,44]. Interestingly, laboratory spectra[45] (1.3 μm to 2.5 μm) of a thin film of crystalline ice deposited at 150 K and cooled down to 16 K show this 1.65 μm crystalline band. On the other hand, crystalline ice formed at higher temperatures does not exhibit this feature, which is also absent in amorphous ice[43]. From the relative intensities of these features and their observed central wavelengths, one could obtain constraints on the formation and current temperature of the observed ices, yet this would also need detailed modelling of the other strong nearby features that affect the shape of the nearby continuum.

Hydrogen peroxide-bearing ice. We observe a subtle 'plateau' at 3.5 μm (Fig. 1), which could be attributed to hydrogen peroxide (H$_2$O$_2$), yet proper recovery of this feature would require accurate modelling of the nearby strong water bands. It is well known that the icy satellites within the Saturnian and Jovian magnetospheres are subjected to intense fluxes of energetic particles that alter their surficial properties and induce many physical and chemical effects[46,47]. However, modelling how efficiently radiation processes affect Enceladus' surface quantitatively will need to account for the relatively low energetic proton fluxes[48,49] and relatively high particle deposition rates of plume fallout[50] experienced by the Saturnian moon. Among the several effects studied in the laboratory is the formation of H$_2$O$_2$ evidenced from the appearance of a band at about 3.5 μm in the spectrum of water ice irradiated with energetic particles[51–53]. This 3.5 μm H$_2$O$_2$ feature has been found on the surface of Europa[54,55], while ultraviolet observations made by

the Galileo Ultraviolet Spectrometer suggest that H_2O_2 may be present on Ganymede and Callisto as well[56]. Consequently, the possible 3.5 μm feature on Enceladus could be consistent with radiolytic generation of H_2O_2 from its H_2O ice rich surface.

CN compounds. A possible absorption is observed near 4.5 μm (Fig. 1) and could be associated to CN and/or (iso)cyanate compounds, yet baseline issues for these low flux continuum levels make this identification only tentative. Radiolytic and photochemical processing of C-containing ices results in the formation of an organic material that, formed at low temperatures, evolves during the heating of the samples and yields an organic refractory material that is stable at room temperature and above[57]. When the original ice contains both C and N atoms, the stable residue exhibits a strong and clear feature centred at about 4.6 μm that effectively reproduces the features observed in some ultra-carbonaceous Antarctic meteorites[58]. That feature is attributed to cyanate and isocyanate bonds and is considered to be evidence for the energetic processing (by photons, electrons or ions) of the ices. Similarly, a feature centred near 4.57 μm was detected on Callisto and attributed to CN-bearing organics[59]. Such ices on Enceladus could be deposited on the surface by micrometeoritic bombardment or by energetic processing of reduced C- and N-bearing materials. Another possibility is that CN compounds might already be present in Enceladus' plume[37], and could then be deposited over the surface.

Data availability

The data used in this analysis are publicly available at the Space Telescope Science Institute (STScI) JWST archive (https://mast.stsci.edu/), programme no. 1250.

Code availability

The retrieval software package used in this study is the Planetary Spectrum Generator, which is free and available online at https://psg.gsfc.nasa.gov (refs. 29,30), with the data-reduction scripts available at https://github.com/nasapsg. Figures were made with Matplotlib version 3.2.1 (ref. 60), available under the Matplotlib license at https://matplotlib.org/.

References

1. Cassidy, T. A. & Johnson, R. E. Collisional spreading of Enceladus' neutral cloud. *Icarus* **209**, 696–703 (2010).
2. Brown, R. H. et al. Composition and physical properties of Enceladus' surface. *Science* **311**, 1425–1428 (2006).
3. Spencer, J. R. et al. Cassini encounters Enceladus: background and the discovery of a south polar hot spot. *Science* **311**, 1401–1405 (2006).
4. Baum, W. A. et al. Saturn's E ring: I. CCD observations of March 1980. *Icarus* **47**, 84–96 (1981).
5. Haff, P. K., Eviatar, A. & Siscoe, G. L. Ring and plasma: the enigmae of Enceladus. *Icarus* **56**, 426–438 (1983).
6. Smith, B. A. et al. A new look at the Saturn system: the Voyager 2 images. *Science* **215**, 504–537 (1982).
7. Shemansky, D. E., Matheson, P., Hall, D. T., Hu, H.-Y. & Tripp, T. M. Detection of the hydroxyl radical in the Saturn magnetosphere. *Nature* **363**, 329–331 (1993).
8. Dougherty, M. K., Buratti, B. J., Seidelmann, P. K. & Spencer, J. R. Enceladus as an active world: history and discovery. in *Enceladus and the Icy Moons of Saturn* (eds Schenk, P. M. et al.) 3–16(University of Arizona Press, 2018); https://doi.org/10.2458/azu_uapress_9780816537075-ch001
9. Hansen, C. J. et al. Enceladus' water vapor plume. *Science* **311**, 1422–1425 (2006).
10. Porco, C. C. et al. Cassini observes the active south pole of Enceladus. *Science* **311**, 1393–1401 (2006).
11. Waite, J. H. et al. Cassini ion and neutral mass spectrometer: Enceladus plume composition and structure. *Science* **311**, 1419–1422 (2006).
12. Spahn, F. et al. Cassini dust measurements at Enceladus and implications for the origin of the E ring. *Science* **311**, 1416–1418 (2006).
13. Dougherty, M. K. et al. Identification of a dynamic atmosphere at Enceladus with the Cassini magnetometer. *Science* **311**, 1406–1409 (2006).
14. Schenk, P. M., Clark, R. N., Howett, C. J. A., Verbiscer, A. J. & Waite, J. H. *Enceladus and the Icy Moons of Saturn* (Univ. Arizona Press, 2018).
15. Hartogh, P. et al. Direct detection of the Enceladus water torus with Herschel. *Astron. Astrophys.* **532**, L2 (2011).
16. Smith, H. T. et al. Enceladus plume variability and the neutral gas densities in Saturn's magnetosphere. *J. Geophys. Res. Space Phys.* https://doi.org/10.1029/2009JA015184 (2010).
17. Waite, J. H. et al. Liquid water on Enceladus from observations of ammonia and 40Ar in the plume. *Nature* **460**, 487–490 (2009).
18. Hansen, C. J. et al. The composition and structure of Enceladus' plume from the complete set of Cassini UVIS occultation observations. *Icarus* **344**, 113461 (2020).
19. Ingersoll, A. P., Ewald, S. P. & Trumbo, S. K. Time variability of the Enceladus plumes: orbital periods, decadal periods, and aperiodic change. *Icarus* **344**, 113345 (2020).
20. Gardner, J. P. et al. The James Webb Space Telescope. *Space Sci. Rev.* **123**, 485–606 (2006).
21. Böker, T. et al. The near-infrared spectrograph (NIRSpec) on the James Webb Space Telescope III. Integral-field spectroscopy. *Astron. Astrophys.* **661**, A82 (2022).
22. Cruikshank, D. et al. A spectroscopic study of the surfaces of Saturn's large satellites: HO ice, tholins, and minor constituents. *Icarus* **175**, 268–283 (2005).
23. Emery, J. P., Burr, D. M., Cruikshank, D. P., Brown, R. H. & Dalton, J. B. Near-infrared (0.8-4.0m) spectroscopy of Mimas, Enceladus, Tethys, and Rhea. *Astron. Astrophys.* **435**, 353–362 (2005).
24. Combe, J.-P. et al. Nature, distribution and origin of CO_2 on Enceladus. *Icarus* **317**, 491–508 (2019).
25. Waite, J. H. et al. Cassini finds molecular hydrogen in the Enceladus plume: evidence for hydrothermal processes. *Science* **356**, 155–159 (2017).
26. Cartwright, R. J. et al. Evidence for ammonia-bearing species on the Uranian satellite Ariel supports recent geologic activity. *Astrophys. J. Lett.* **898**, L22 (2020).
27. Zheng, W., Jewitt, D. & Kaiser, R. I. Infrared spectra of ammonia–water ices. *Astrophys. J. Suppl. S.* **181**, 53 (2009).
28. Roser, J. E., Ricca, A., Cartwright, R. J., Ore, C. D. & Cruikshank, D. P. The infrared complex refractive index of amorphous ammonia ice at 40K (1.43–22.73 μm) and Its relevance to outer Solar System bodies. *Planet. Sci. J.* **2**, 240 (2021).
29. Villanueva, G. L., Smith, M. D., Protopapa, S., Faggi, S. & Mandell, A. M. Planetary Spectrum Generator: an accurate online radiative transfer suite for atmospheres, comets, small bodies and exoplanets. *J. Quant. Spectrosc. Radiat. Transf.* **217**, 86–104 (2018).
30. Villanueva, G. L. et al. *Fundamentals of the Planetary Spectrum Generator* (NASA Goddard Space Flight Center, 2022).
31. Villanueva, G. L. et al. Water in planetary and cometary atmospheres: H_2O/HDO transmittance and fluorescence models. *J. Quant. Spectrosc. Radiat. Transf.* **113**, 202–220 (2012).
32. Villanueva, G. L., Disanti, M. A., Mumma, M. J. & Xu, L.-H. A quantum band model of the v_3 fundamental of methanol (CH_3OH) and its application to fluorescence spectra of comets. *Astrophys. J.* **747**, 37 (2012).

33. Villanueva, G. L., Mumma, M. J. & Magee-Sauer, K. Ethane in planetary and cometary atmospheres: transmittance and fluorescence models of the v_7 band at 3.3 μm. *J. Geophys. Res.* https://doi.org/10.1029/2010JE003794 (2011).

34. Hansen, C. J. et al. Water vapour jets inside the plume of gas leaving Enceladus. *Nature* **456**, 477–479 (2008).

35. Teolis, B. D. et al. Enceladus plume structure and time variability: comparison of Cassini observations. *Astrobiology* **17**, 926–940 (2017).

36. Huebner, W. F., Keady, J. J. & Lyon, S. P. Solar photo rates for planetary atmospheres and atmospheric pollutants. *Astrophys. Space Sci. (ISSN 0004-640X)* **195**, 1–289 (1992).

37. Postberg, F. et al. Plume and surface composition of Enceladus. in *Enceladus and the Icy Moons of Saturn* (eds Schenk, P. M. et al.) 129–162 (University of Arizona Press, 2018); https://doi.org/10.2458/azu_uapress_9780816537075-ch00

38. Glein, C. R. & Waite, J. H. The carbonate geochemistry of Enceladus' ocean. *Geophys. Res. Lett.* **47**, e2019GL085885 (2020).

39. Pinto, O. H., Womack, M., Fernandez, Y. & Bauer, J. A survey of CO, CO_2, and H_2O in comets and centaurs. *Planet. Sci. J.* **3**, 247 (2022).

40. Ootsubo, T. et al. AKARI near-infrared spectroscopic survey for CO_2 in 18 comets. *Astrophys. J.* **752**, 15 (2012).

41. MacKenzie, S. M. et al. The Enceladus orbilander mission concept: balancing return and resources in the search for life. *Planet. Sci. J.* **2**, 77 (2021).

42. Rodgers, C. D. *Inverse Methods for Atmospheric Sounding: Theory and Practice* (World Scientific, 2000); https://doi.org/10.1142/3171

43. Mastrapa, R. M. et al. Optical constants of amorphous and crystalline H_2O-ice in the near infrared from 1.1 to 2.6 μm. *Icarus* **197**, 307–320 (2008).

44. Mastrapa, R. M., Sandford, S. A., Roush, T. L., Cruikshank, D. P. & Ore, C. M. D. Optical constants of amorphous and crystalline H_2O-ice: 2.5–22 μm (4000–455 cm^{-1}). *Astrophys. J.* **701**, 1347 (2009).

45. Leto, G., Gomis, O. & Strazzulla, G. The reflectance spectrum of water ice: is the 1.65 mu msp peak a good temperature probe? *Mem. della Soc. Astronomica Ital. Suppl.* **6**, 57 (2005).

46. Strazzulla, G. Cosmic ion bombardment of the icy moons of Jupiter. *Nucl. Instrum. Methods Phys. Res., Sect. B* **269**, 842–851 (2011).

47. Bennett, C. J., Pirim, C. & Orlando, T. M. Space-weathering of Solar System bodies: a laboratory perspective. *Chem. Rev.* **113**, 9086–9150 (2013).

48. Roussos, E. et al. Discovery of a transient radiation belt at Saturn. *Geophys. Res. Lett.* **35**, L22106 (2008).

49. Kollmann, P. et al. Spectra of Saturn's proton belts revealed. *Icarus* **376**, 114795 (2022).

50. Southworth, B. S., Kempf, S. & Spitale, J. Surface deposition of the Enceladus plume and the zenith angle of emissions. *Icarus* **319**, 33–42 (2019).

51. Moore, M. H. & Hudson, R. L. IR detection of H_2O_2 at 80 K in ion-irradiated laboratory ices relevant to Europa. *Icarus* **145**, 282–288 (2000).

52. Gomis, O., Satorre, M. A., Strazzulla, G. & Leto, G. Hydrogen peroxide formation by ion implantation in water ice and its relevance to the Galilean satellites. *Planet. Space Sci.* **52**, 371–378 (2004).

53. Loeffler, M. J., Raut, U., Vidal, R. A., Baragiola, R. A. & Carlson, R. W. Synthesis of hydrogen peroxide in water ice by ion irradiation. *Icarus* **180**, 265–273 (2006).

54. Carlson, R. W. et al. Hydrogen peroxide on the surface of Europa. *Science* **283**, 2062–2064 (1999).

55. Trumbo, S. K., Brown, M. E. & Hand, K. P. H_2O_2 within chaos terrain on Europa's leading hemisphere. *Astron. J.* **158**, 127 (2019).

56. Hendrix, A. R., Barth, C. A., Stewart, A. I. F., Hord, C. W. & Lane, A. L. *Hydrogen Peroxide on the Icy Galilean Satellites* (Lunar and Planetary Insitute, 1999); https://www.lpi.usra.edu/meetings/LPSC99/pdf/2043.pdf

57. Accolla, M. et al. Combined IR and XPS characterization of organic refractory residues obtained by ion irradiation of simple icy mixtures. *Astron. Astrophys.* **620**, A123 (2018).

58. Baratta, G. A. et al. Organic samples produced by ion bombardment of ices for the EXPOSE-R2 mission on the International Space Station. *Planet. Space Sci.* **118**, 211–220 (2015).

59. McCord, T. B. et al. Organics and other molecules in the surfaces of Callisto and Ganymede. *Science* **278**, 271–275 (1997).

60. Caswell, T. A. et al. matplotlib/matplotlib v.3.1.3. *Zenodo* https://doi.org/10.5281/zenodo.3633844 (2020).

Acknowledgements

Author contributions
G.L.V., H.B.H., S.N.M., K.P.H., L.P., J. Spencer, J. Stansberry and G.S. designed the observations and prepared the observational plans. G.L.V., V.K., S.F., R.C., J. Stansberry, B.H., S.P., G.L., M.H. and K.D. analysed the data, extracted calibrated spectra, produced maps and performed retrievals. C.R.G., L.R., N.R.-G., G.C.-M. and M.E.M. assisted with the interpretation of the results and provided context to related mission and astronomical investigations. All of the authors contributed to the preparation, writing and editing of the manuscript.

Competing interests
The authors declare no competing interests.

Additional information

Article

¹NASA Goddard Space Flight Center, Greenbelt, MD, USA. ²Association of Universities for Research in Astronomy, Washington, DC, USA. ³American University, Washington, DC, USA. ⁴Southwest Research Institute, San Antonio, TX, USA. ⁵Carl Sagan Center for Research at the SETI Institute, Mountain View, CA, USA. ⁶KTH Royal Institute of Technology, Stockholm, Sweden. ⁷Jet Propulsion Laboratory, Pasadena, CA, USA. ⁸NASA Headquarters, Washington, DC, USA. ⁹Southwest Research Institute, Boulder, CO, USA. ¹⁰Space Telescope Science Institute, Baltimore, MD, USA. ¹¹Department of Astronomy & CRESST II, University of Maryland, College Park, MD, USA. ¹²INAF-Osservatorio Astrofisico di Catania, Catania, Italy. ¹³Università degli Studi della Basilicata, Potenza, Italy. ¹⁴Universite Paris-Saclay, Orsay, France. ¹⁵Cornell Center of Astrophysics and Planetary Sciences, Ithaca, NY, USA. ¹⁶University of Idaho, Moscow, ID, USA. ✉e-mail: geronimo.villanueva@nasa.gov
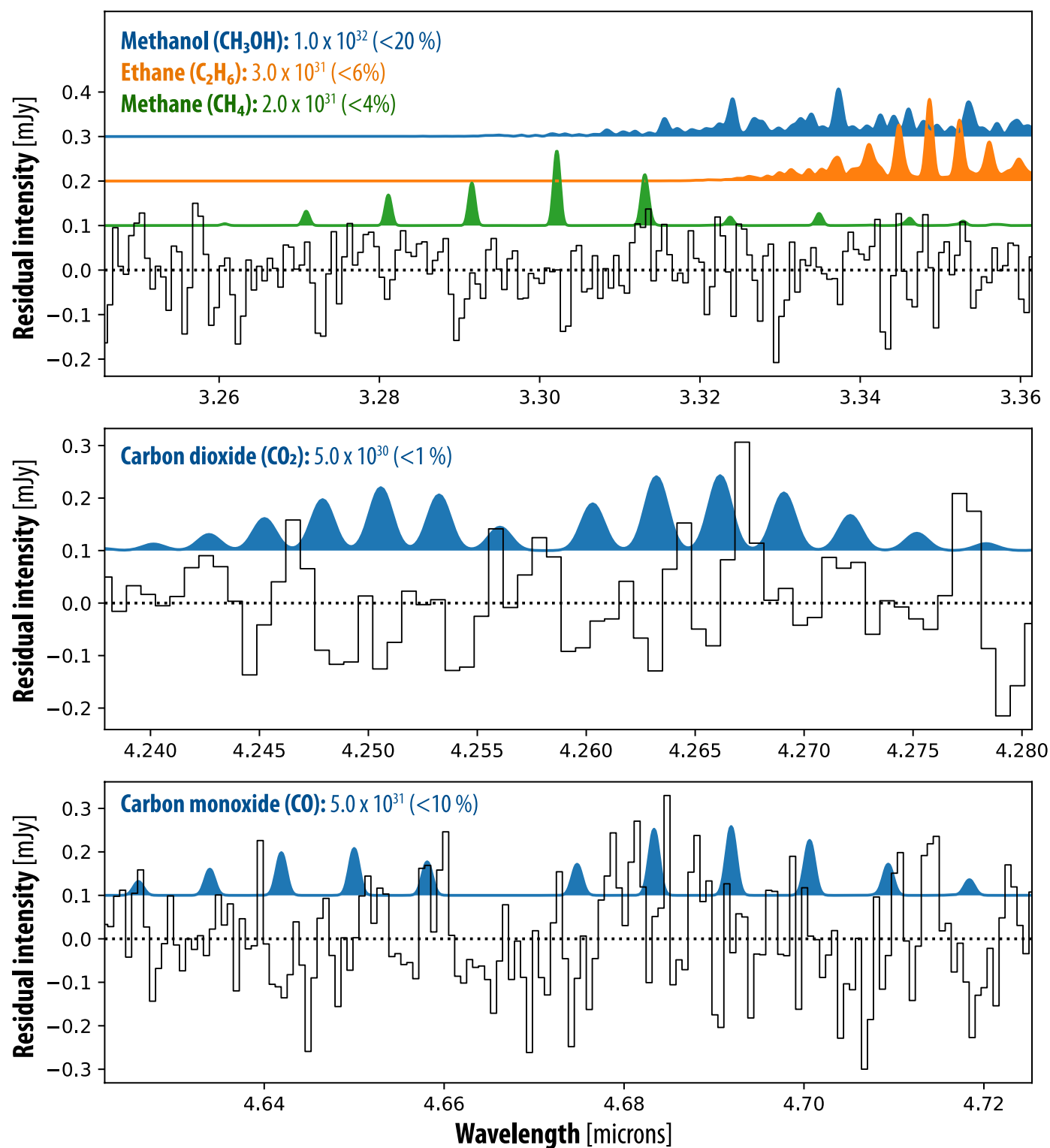
Extended Data Fig. 1 | Searches for organic species in the plume of Enceladus. Residual spectra for three spectral regions in which CH₃OH, C₂H₆, CH₄, CO₂ and CO molecular emission were searched. The spectra were integrated across the plume region. The models are at the 3s level in number of molecules and were computed assuming a rotational temperature of 25 K as for water.